Trigger Note # 1. PHOBOS Trigger Counters

E. J. Garcia-Solis, A. C. Mignerey, L. Remsberg

July 23, 1998

1 Overview

Phobos is a detector designed to study the physics of ultra-relativistic heavy-ion collisions accessible at the Relativistic Heavy Ion Collider (RHIC) at Brookhaven National Laboratory [1]. The Phobos system was conceived to look for signatures of new states of nuclear matter produced under conditions of extremely high baryon density. Figure 1 illustrates the essential features of Phobos. The system consists of multiplicity and pseudorapidity detectors, a silicon based magnetic spectrometer that provides particle identification and tracking for kaons, pions and protons, and the trigger system.

The spectrometer is able to identify particles with transverse momenta down to 30 MeV/c, in the central pseudorapidity window of $0. < \eta < 5.3$. The multiplicity and pseudorapidity detectors are arrays of silicon strip detectors surrounding the interaction region and a set of circular pads located along the beam line. The detection system is complemented with trigger counters that further extend the pseudorapidity coverage and provide event selction the for the data acquisition.

2 Trigger Geometry

Several criteria determined the geometry of the trigger counters; the physical limits and physics requirements of the PHOBOS detector, the desired coverage, the triggering efficiency, and the availability and cost of the components. Based on these considerations, and on the simulations described in the next section, we have converged to the present design of the trigger counters.

There are two set of counters to provide a first-level minimum bias trigger. The *ring counters* are two sets of 16 Cerenkov radiators arranged in a ring around the beam pipe. These counters detect the occurrence of an interaction and give a crude measurement of the beam-crossing location. Each Cerenkov module is a 4×2.5 cm cylinder made of UVT plastic (BC-800) glued to a R1924 Hamamatsu phototube. In front of each module, a 0.5 radiation length lead disk

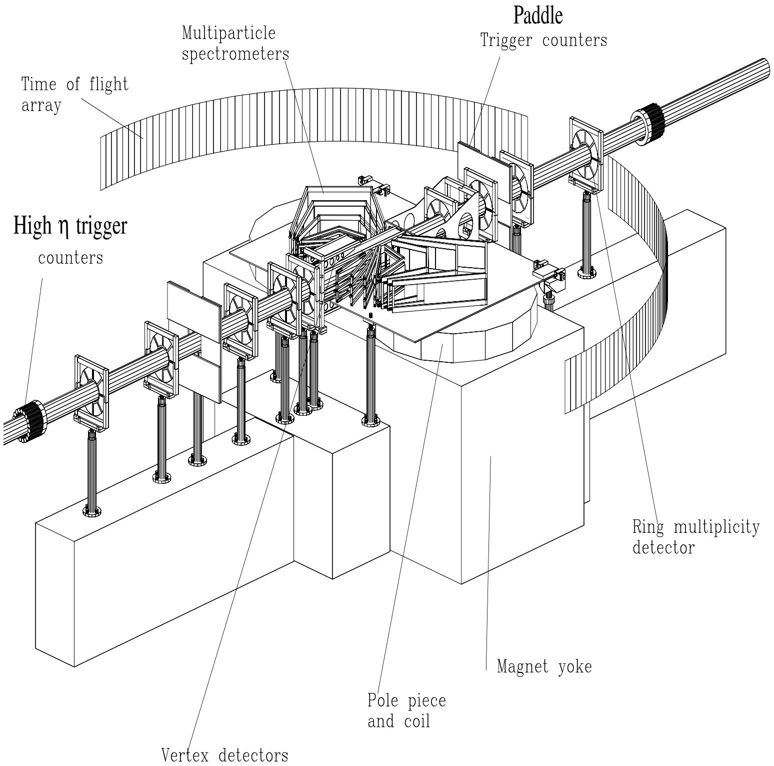

Figure 1:
The PHOBOS detector, perspective view.

will be included to detect π_o via photon conversion. Figure 2 is a drawing of these counters.

The other set of trigger counters are the *paddle counters*. These detectors are closer to the interaction region and also centered along the beam line. The paddle counters are two arrays of 16 scintillators forming a disk. Each disk is positioned at opposite sides of the interaction region, and perpendicular to the beam axis. Each paddle, is made of Bicron BC404 scintillator attached via a Plexiglas light guide to a single Hamamatsu R329-02 photomultiplier tube. The dimensions of each paddle are shown in Fig. 3. The paddle counters are designed to trigger peripheral collisions and to give a first approximation of the event centrality.

For the trigger design, the relevant elements of the PHOBOS detector are the extent of the beam pipe and the dimensions and locations of the multiplicity disk detectors. The beam pipe is a Be tube of 5-cm exterior radius and 12-m long. The 5-cm interior radius and 11 cm exterior radius silicon disks are located at ± 112, ± 234 and ± 504 cm from the interaction point. In order to avoid shadowing these detectors, the paddle counters are located at $z = \pm 321$ cm from the interaction point. On the other hand the ring counters are set at $z = \pm 557$ cm, to achieve the highest possible η coverture. The location of the trigger counters along the beam pipe is shown in Fig. 4.

Given the distence from the center of the interaction region and the dimensions of the trigger counters, the pseudorapidity coverage of the paddle counters is $\eta = \pm 3.7 \ to \ \pm 4.5$, and ring counters is $\eta = \pm 4.9 \ to \ \pm 5.3$.

3 Trigger Simulations

3.1 Au + Au

The set of events for the simulation of the system Au + Au at 200 GeV/A was generated with the code HIJET [2]. These events were used as an input of the Phobos Monte Carlo (PMC), a GEANT based tracking library. Provided the right geometry set up, the PMC output delivers, among other things, the hit distribution of every particle, primary or secondary. With this information and using analysis codes based on ROOT, it is possible to set the gates and conditions necessary to study the response of the trigger counters.

Figure 5 shows the energy deposited in one module of the ring and paddle counters from several minimum bias Au + Au events. The particles that cross the modules deposit an average of 1.7 and 6.2 MeV for the paddles and ring modules (*rings*), respectively. The hits with lower energy are either particles created inside the counter or particles that do not cross entirely the counters. It is possible to define a hit in the trigger modules when a particle deposits more than $\Delta E_{cut} = 1.2 MeV$ for the paddles and $\Delta E_{cut} = 6.2 MeV$ for the rings. Note that for the ring counters this is an approximation since, for the purpose

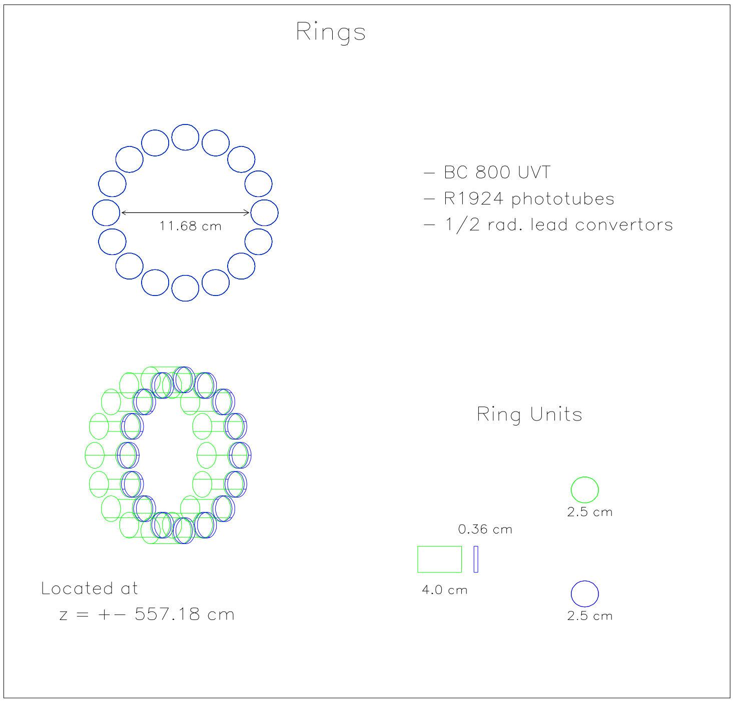

Figure 2:
Ring counters.

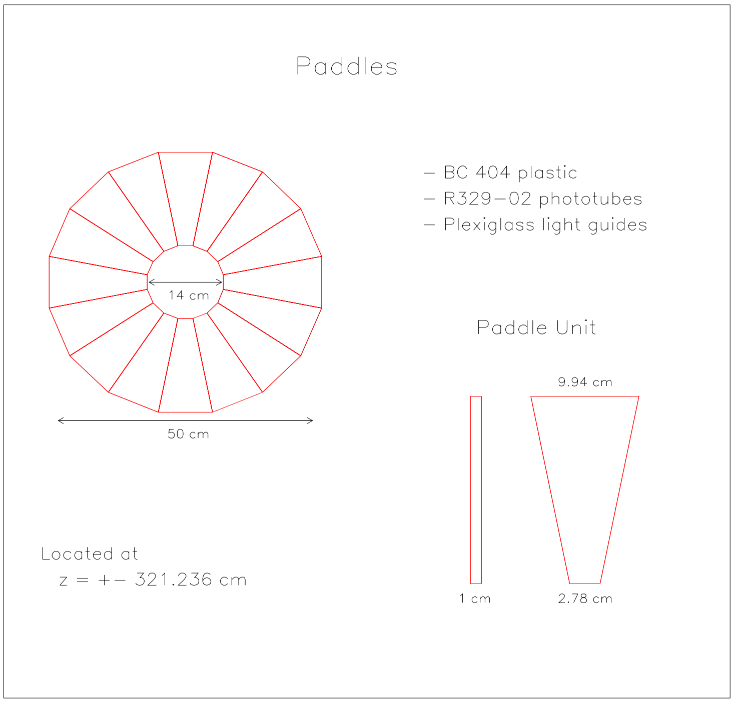

Figure 3:
Paddle counters.

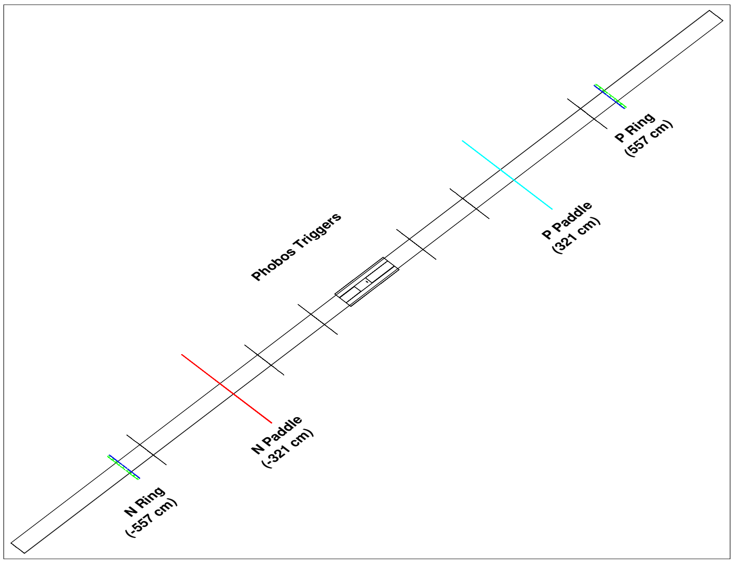

Figure 4:
The location of the trigger counters along the beam pipe. In this picture the interaction region is located at Z = 0.

of the simulation, the ring material is plastic scintillator. A similar response (but with a different energy scale) from Cerenkov radiators is expected.

Whenever there is a gold-gold interaction, there are two useful variables that can be extracted from the hit information in the counters, the number of hits in each module (*multiplicity*) and the number of modules hit (*occupancy*). These variables depend on the degree of centrality of the interaction, so that the response of the triggers has to be studied as a function of the impact parameter.

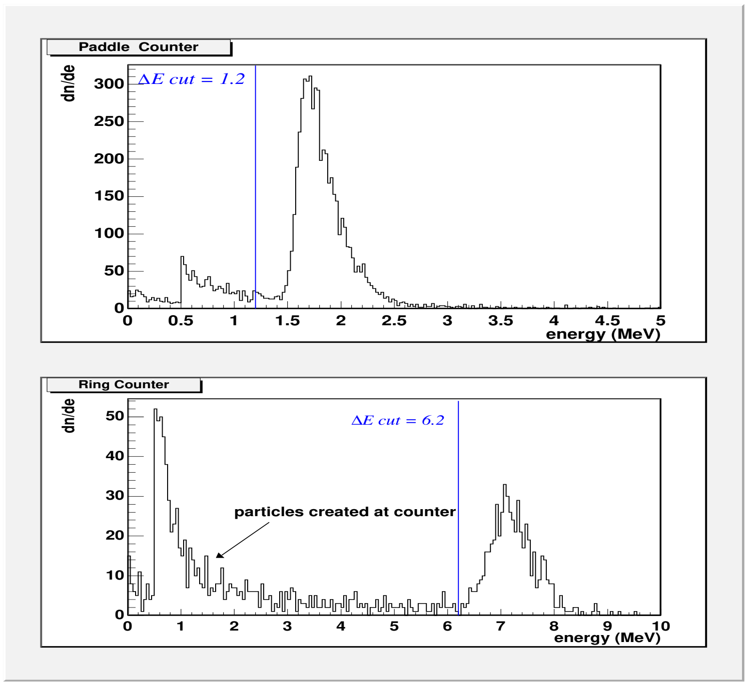

Figure 5:
Energy deposited in one module of the ring and paddle counter.

The events were generated from HIJET for impact parameters varying from zero to the grazing distance (15 fm). The distribution of hit (as defined by the cuts in Fig. 5) multiplicity and hit occupancy were then generated. The profile (mean and rms) of these distributions are shown in Figs. 6 to 9. The average multiplicity of the paddle modules is plotted in Fig. 6 . The mean multiplicity is 50 for zero impact parameter and decreases down to zero for the most peripheral events. This variable permits event selection by centrality of 30% corresponding to $b \simeq 8$ fm. Using different multiplicity cuts, the average occupancy of the paddle counters is plotted as a function of the impact parameter in Fig. 7. The 16 modules of each array are hit in every interaction up to $b \simeq 9$ fm. After this point the occupancy decreases sharply, depending on the multiplicity cut.

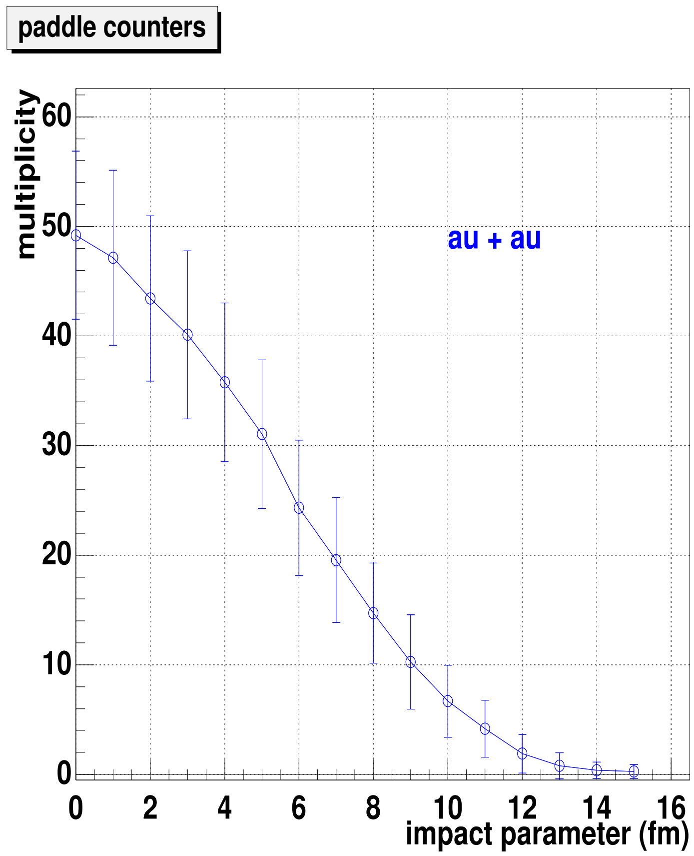

Figure 6:
Paddle Counter multiplicity.

The average multiplicity in the ring modules as a function of the centrality is shown in Fig. 7. Requiring a minimum multiplicity cut of 1, the ring counters are able to discriminate interactions up to $b \simeq 8$ fm (around 30% centrality). The average occupancy for the rings is shown in Fig. 7, the mean occupancy allows discrimination up to a centrality of 25 to 30 %, depending on

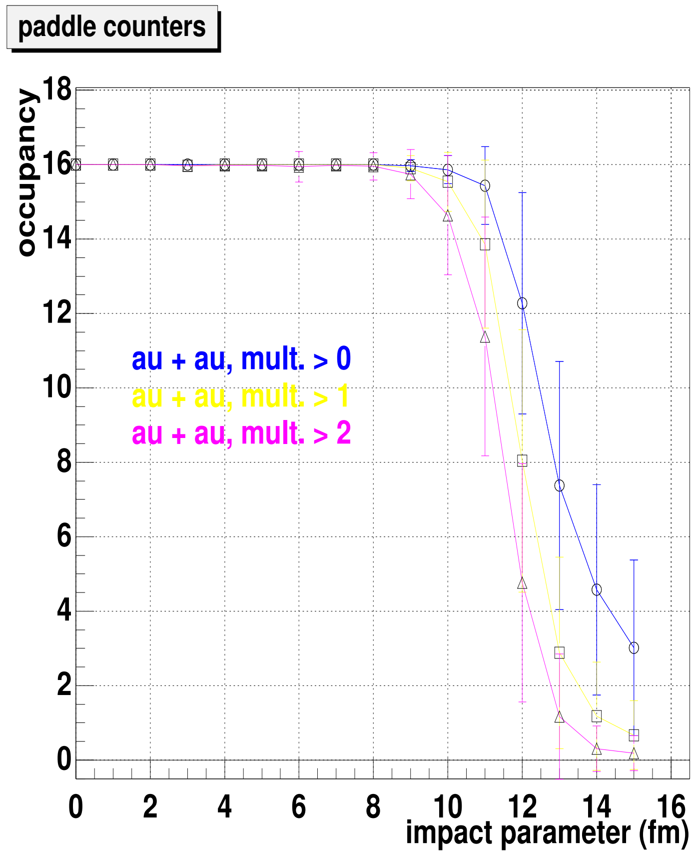

Figure 7:
Paddle Counter occupancy.

the multiplicity cut.

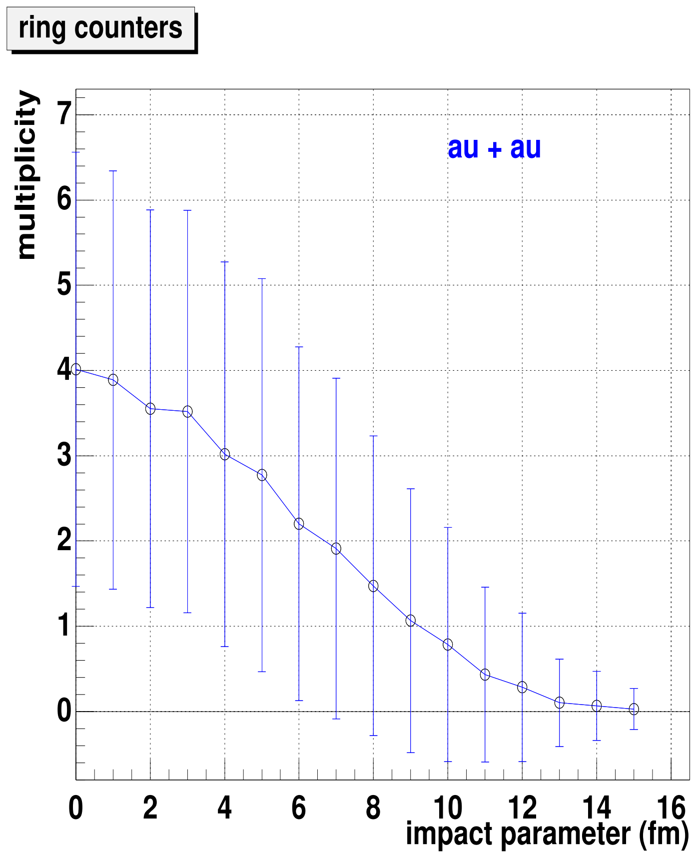

Figure 8:
Ring counter multiplicity.

Finally, integrating over all impact parameters, it was found for the paddle counters $\overline{occupancy} = 15.9 \pm 0.11$, $\overline{multiplicity} = 21.63 \pm 12.63$, and for the ring counters $\overline{occupancy} = 11.30 \pm 3.1$, $\overline{multiplicity} = 2.10 \pm 2.19$.

3.2 Background

There are two kinds of background that may have an effect on the performance of the trigger counters; the background produced from particles that come from some process other than the beam-beam interaction (machine background), and

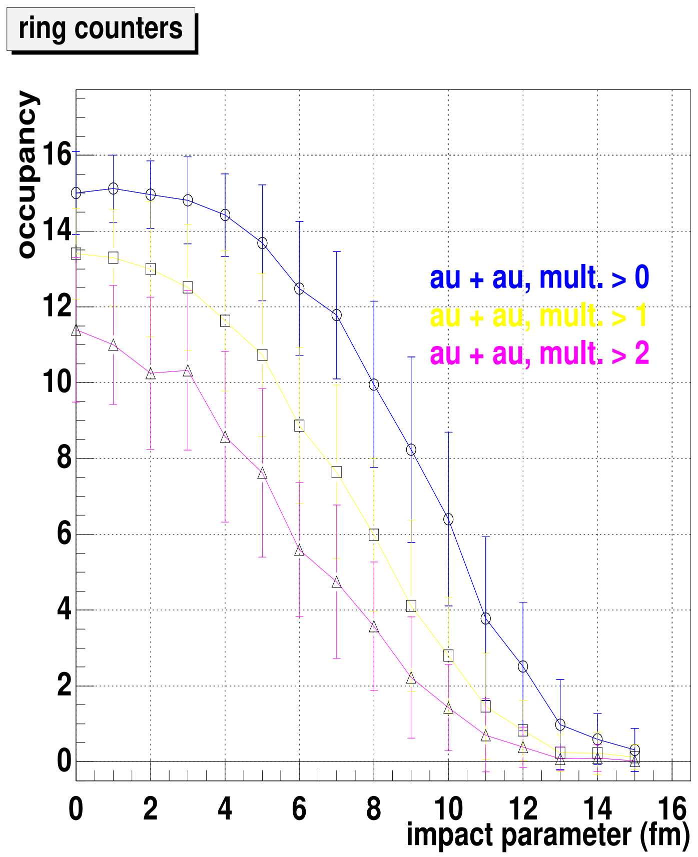

Figure 9:
Ring counter occupancy.

the background coming from the beam-beam interactions. Possible sources of machine background are scattering from collimators, beam gas interactions in the experimental region, beam gas interactions in the upstream straight sections, and DC beam - DC beam interactions. Sources of interac

tion backgrounds are hadronic interactions (interactions with the detector materials) and e+e- production.

With the exception of the beam gas interactions in the experimental region, it is difficult to asses a priori the magnitude of the machine background. An overview of recent studies of the RHIC background environment can be found in ref. [3]. The background from interactions with the detector materials are included in the PMC, therefore only the e+e- interaction and the beam gas background are particularly considered in this review. The major parameters for RHIC used in this paper are discussed in reference [4].

3.2.1 Beam Gas Background

This is the background coming from interactions of the beam with residual gas ions in the beam pipe. At around 10^{-9} Torr of pressure the gas composition in the beam pipe is expected to be 95 % $He + 5$ % $H_2 \simeq 100$ % He, from which it is possible to calculate the gas density (ρ):

$$\rho = \frac{P}{kT} \tag{1}$$

$$\rho = 9.66\ 10^{+18}\ \frac{P(Torr)}{T(K)}, \tag{2}$$

where k is the Boltzmann constant. Assuming $T \simeq 292.72$ K, will have $\rho = 3.3 \times 10^{16}\ P(Torr)$ molecules/cm^3. On the other hand, the geometrical cross section

$$\sigma = \pi\ r_0\ ({A_1}^{1/3} + {A_2}^{1/3})^2 \tag{3}$$

$$\sigma_{Au+He} = 2.7\ barns = 2.7 \times 10^{-24}\ cm^2, \tag{4}$$

so that the probability of beam gas interactions per crossing is given by

$$f_{Au+He} = N_{Au}\ l\ \rho\ \sigma_{Au+He}\ \simeq 10^{-5}, \tag{5}$$

where $N_{Au} \simeq 10^9$, the number of gold molecules per crossing, and l is the beam pipe longitude $\simeq 10$ m. The beam gas rate (number of interactions per crossing per second) is

$$R_{Au+He} = \nu\ 2\ f_{Au+He}, \tag{6}$$

with ν the RHIC frequency. The factor of two is included to take into account two beams. With

$$\nu = \frac{number\ of\ bunches\ per\ cycle}{cycle\ period} \quad (7)$$

$$\nu = \frac{57}{12.810^{-6}} \quad (8)$$

$$\nu = 4.5 \times 10^6\ Hz, \quad (9)$$

so that $R_{Au+He} \simeq 800$ Hz. Note that this rate is comparable to the "physics" rate:

$$R_{Au+Au} = L\ \sigma_{Au+Au} = 1329\ Hz, \quad (10)$$

assuming an average nominal luminosity $L = 2 \times 10^{26}$ cm^{-2}/s^{-1}. It is possible to simulate the beam gas interactions using the PMC. This was done by using HIJET to generate several events or interactions (at random impact parameters) and then randomly locating the interaction vertex along the beam pipe.

For any event where the paddle counters are hit (the condition $mult. > 0$) the multiplicity on each module is 2.02 ± 1.38, and the mean array occupancy is 8 ± 8. For the ring counters, the mean multiplicity is 1.7 ± 1.31, and the mean occupancy 2.7 ± 1.8. To calculate this occupancy the lowest multiplicity condition was also used ($mult. > 0$). Note that these number are averages only for "interaction" events, a true counter background rate would have to combine beam gas interaction rate with the physics rate. Also as shown in the next section these events are not likely to produce triggers.

3.2.2 e+ e- Background

During the beam crossing in a relativistic heavy-ion collider, the Lorentz-contracted peripheral Coulomb field is sufficiently intense to induce pair production. The production of electron-positron pairs has been studied over a long time. A detailed analysis of this process in the RHIC environment can be found in [5] and [6]. The probability distribution for N-pair production is given by a Poisson distribution:

$$P(b) = P(b)^N \frac{exp[-P(b)]}{N!} \quad (11)$$

the probability $P(b)$ is approximated to first order by the equation:

$$P(b) \simeq \frac{14}{9\pi}(Z^2\alpha^2)^2 \frac{\lambda_c}{\pi b}^2 ln^2(\frac{\gamma\delta\lambda_c}{2b}) + \Delta(Z), \quad (12)$$

where b is the impact parameter, $\gamma = 2 \times 10^4$ is the ion energy, δ is a constant, $Z = 79$ is the ion charge, $\lambda_c = 386$ fm is the reduced Compton wave length of the electron, and α is the fine-structure constant. Using Eq. (12) it is possible to calculate the pair production cross section:

$$
\begin{aligned}
\sigma_{1\ pair} &= 32.3 \times 10^3 b & (13)\\
\sigma_{2\ pair} &= 1.96 \times 10^3 b & (14)\\
\sigma_{3\ pair} &= 437 \times b & (15)\\
\sigma_{4\ pair} &= 114 \times b & (16)\\
\sigma_{5\ pair} &= 28 \times b & (17)
\end{aligned}
$$

The one and two pair production rates are then

$$
\begin{aligned}
R_{1\ e+e-} &= L\ \sigma_{1pair} = 6.6\ MHz & (18)\\
R_{2\ e+e-} &= L\ \sigma_{2pair} = 0.4\ MHz, & (19)
\end{aligned}
$$

which gives an average of about $\overline{n} \simeq 1.6$ pairs produced per crossing. The probability of no pairs produced can be estimated by,

$$
\begin{aligned}
P(N) &\simeq \frac{\overline{n}^N exp(\overline{n})}{N!} & (20)\\
P(0) &\simeq exp(-1.70) = 0.20 & (21)
\end{aligned}
$$

The pair production process was simulated with the PMC using an event generator written by M. Fatyga, incorporated to PHENIX's PISA [7] by C. Maguire and A. Rose. This program is able to reproduce the pair distributions described in ref. [5] and [6]. The event generator randomly selects the impact parameter of interaction. The rapidity of the pair is also randomly selected, limited by the pair's invariant mass. For the kinematics of the pairs, the generator assigns randomly the azimuthal distribution of the positrons, and then $\phi_{e+} = \phi_{e-} + \pi$. For the transverse momentum ${p_t}^{e+} = -{p_t}^{e-}$. In the simulation the pairs were produced at the interaction point, then propagated by the PMC.

For the paddle counters a mean multiplicity from the pair production is 1.101 ± 0.10, and a mean array occupancy of 1.04 ± 0.18 (with lowest multiplicity condition $mult. > 0$). For the ring counters, the mean multiplicity was 1.0, and the mean occupancy 1.0, with $mult. > 0$. Note that these numbers are not strict averages; they are averages only for "interaction" events. Also, as shown in the next section, these events are not likely to produce event triggers, but serve as an underleying background for the real triggers.

3.3 Triggering

3.3.1 Trigger Efficiencies

One of the main concerns in the design of the trigger counters is their efficiency. For example, it is important to make sure that the efficiency among the two sets of detectors is complementary as a function of the centrality. To this end a Monte Carlo study was done. A set of events for the reaction Au + Au at 200 GeV was generated with the code HIJET for impact parameters varying from zero to the grazing impact (around 15 fm). These events were used as an input of the PMC.

Once the PMC is ran for different centralities (impact parameters), it is possible to define the efficiency of the paddle or ring counters as:

$$\epsilon = \frac{number\ of\ triggers}{total\ number\ of\ events\ (or\ interactions).} \tag{22}$$

A detector is triggered when both the upstream and downstream elements of the counters meet a trigger condition defined by a limit in the occupancy *and* the multiplicity, within a coincidence window.

Figures 10 and 11 display the efficiency as a function of the impact parameter for the paddles and ring η counters respectively. The efficiency of the detectors was calculated for two trigger conditions. The condition $mult. > 0.$ and $occ. > 0$ is the minimum possible requirement for a trigger, and the other condition is set so that the triggering is above background.

The paddle counters have an efficiency of 1 up to $b = 12$ fm (about 75 % centrality). After that point the efficiency decreases sharply down to about 0.53 for $mult. > 0$ and $occ. > 0$, and down to 0.42 for $mult > 1$ and $occ. > 3$. The ring counters have an efficiency of 1 up to $b = 8\ fm$ (about 30 % centrality), after that point the efficiency decreases.

3.3.2 Trigger Rates

The triggering rates can be calculated using the interaction rates and the trigger information provided by the the Monte Carlo simulation.

$$R = \frac{number\ of\ interactions\ per\ crossing}{second} \tag{23}$$

$$\epsilon = \frac{number\ of\ triggers}{number\ of\ interactions} \tag{24}$$

$$Triggering\ Rate = TR = R\,\epsilon \tag{25}$$

$$TR = \frac{number\ of\ triggers}{second}. \tag{26}$$

From the simulations the “background efficiency”, is displayed in Table 1. These efficiencies were calculated using the “above of background” triggering conditions. For the pair production 10^5 events were simulated, for the beam gas two thousand events were simulated.
using Eq. (26) the triggering rates are calculated (Table 2).
It must be noted that the rates represent an upper limit since there is yet another triggering condition to be considered. That is the rough vertex or timing cut

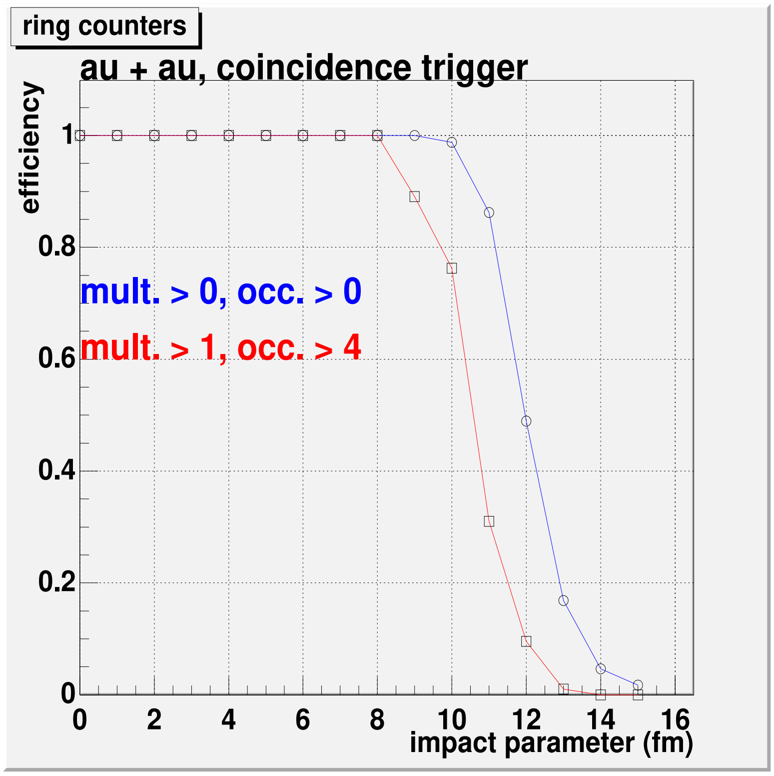

Figure 10:
Ring Counter Efficiency.

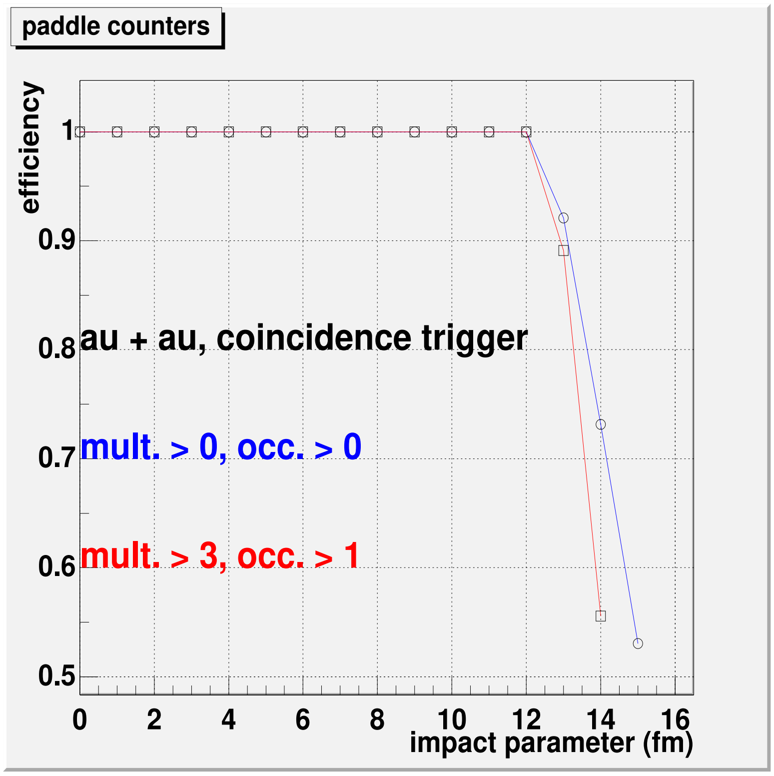

Figure 11:
Paddle Counter Efficiency.

Table 1: Background trigger efficiency.

Efficiency	Paddles	Rings
$\epsilon_{Beam\ Gas}$	0.125	0.002
ϵ_{e+e-}	10^{-5}	10^{-5}

Table 2: Triggering rates.

Triggering Rate	Paddles	Rings
$TR_{Beam\ Gas}$	100 Hz	1.6 Hz
TR_{e+e-}	8 Hz	8 Hz

cut. For example, is expected that most of the beam gas events will be outside of a vertex cut of about 5 ns for the paddle counters, and 300 ps for the ring counters.

4 Design Considerations

4.0.3 Paddle counters, Phototubes Dynamic Range

Since a large number of particles will hit the paddle counter, this will put a constraint in the properties of the phototube to be used. Table 3 shows the characteristics of the phototube Hamamatsu R329-02.

Table 3: Hamamatsu R329-02 characteristics.

G	$5\ \times 10^3$ to $1.0\ \times 10^7$
${V_{applied}}^{max}$	2500 V
I_{max}	20 μA
T_t	48 ns
R_t	2.6 ns

For a standard phototube, it is possible to approximate the anode charge (Q) produced by the number of MIPs (minumum ionizing particles) crossing the scintillators ($\#MIP$):

$$Q = \#MIP \ \Delta E \ C_\epsilon \ Q\mathcal{E} \ G \ S\mathcal{E} \ e \quad (27)$$

where $\Delta E \simeq 1.7\ MeV$ is the energy loss in plastic, $C_\epsilon \simeq 0.10$ is the paddle collection efficiency, $Q\mathcal{E} \simeq 0.0.25$ is the phototube quantum efficiency, G is the phototube gain, $S\mathcal{E} \simeq 10^{-2}\ (\mathrm{eV})^{-1}$ is the scintillator efficiency, and $e = 1.6022 \times 10^{19}$ coulombs. From Eq. (27),

$$Q = 1.3869 \times 10^{-16} \ \#MIP \ G \ coulombs. \quad (28)$$

so that the averaged current is given by

$$\overline{I} = 1.3869 \times 10^{-16} \ \#MIP \ G \ \nu. \quad (29)$$

Taking the standard R329-02 gain of 1.1×10^6, the RHIC frequency, and

$$\begin{aligned}
\#MIP &= 33\ f_{Au+Au} + 3.0\ f_{Beam\ Gas} + 2\ f_{e+e-}, && (30)\\
\overline{I} &\simeq 1.53\ 10^{-10}\ (33\ R_{Au+Au} + 3.0\ R_{Beam\ Gas} + 2\ R_{e+e-}) && (31)\\
\overline{I} &\simeq 2.02\ \mu A, && (32)
\end{aligned}$$

within the required specifications ($\overline{I} < \overline{I}_{max}$). Furthermore, it is possible to calculate the operational voltage range,

$$\begin{aligned}
V &= \frac{Q(50\ \Omega)}{R_t} && (33)\\
V &\simeq 0.029\ \#MIP\ volts. && (34)
\end{aligned}$$

Using $G = 1.1 \times 10^4$, V(1)= 0.029 mV and V(50) = 1.4 V.

4.0.4 High η counters, Phototubes Dynamic Range

For the high η counters, Table 4 shows the characteristics of the phototubes (Hamamatsu R1924-03) to be used.

Table 4: Hamamatsu R1924-03 characteristics.

G	5.0×10^4 to 5.0×10^6
${V_{applied}}^{max}$	$1200\ V$
$\overline{I}_{max}$	$20\ \mu A$
T_t	$19\ ns$
R_t	$2.0\ ns$

The index of refraction for the the Cerenkov radiator to be used with this counters (BC-800) is n = 1.49, then using

$$cos(\theta) = \frac{1}{\beta\, n}, \tag{35}$$

with $\beta \simeq 1$ the relative velocity of the particle, the Cerenkov angle is $\theta = 47.84$ degrees. On the other hand, assuming the wave length interval of 350 to 500 nm corresponding roughly to the response range of the phototubes,

$$\begin{aligned} \frac{dE}{dx} &= 1180 sin(\theta)^2 \simeq 631 ev/cm, & (36) \\ \frac{dn_{p.e}}{dx} &= 390 sin(\theta)^2 \simeq\ 200\ photons/cm, & (37) \end{aligned}$$

so that for the 4 cm long radiator, will have an energy loss of 2.52 MeV, and 836 photons produced. Then the anode charge in the tubes will be

$$Q = \#MIP\ G\ 835\ QE\ e = 3.34\ \times 10^{-17}\ \#MIP\ G\ coulombs, \tag{38}$$

where as in Eq. 27, $QE \simeq .25$ is the quantum efficiency, e the electron charge and G the gain of the tube, and $\#MIP$ the average number of minimum ionizing particles hitting the radiator. Then

$$\begin{aligned} V &= \frac{Q(50\ \Omega)}{R_t} & (39) \\ V &\simeq 0.185\ \#MIP\ volts. & (40) \end{aligned}$$

Using $G = 2.2 \times 10^5$, V(1)= 0.185 mV and V(8) = 1.48 V.

4.0.5 Plastics Radiation Damage

To assess the radiation damage it is possible to calculate from the simulations and the interaction rates the radiation dose deposited in the paddle counters, ring counters and ring counters cement joints.

The year interaction rate is given by

$$\begin{aligned} YR &\simeq 3.152 \times 10^7\ R\ \frac{int.}{year} & (41) \\ YR_{Au+Au} &\simeq 4.28 \times 10^{10} & (42) \\ YR_{Beam\ Gas} &\simeq 2.52 \times 10^{10} & (43) \\ YR_{e+e-} &\simeq 2 \times 10^{14} & (44) \end{aligned}$$

so that the number of MIP interacting in the counters per year is:

$$
\begin{aligned}
Y\#MIP_{paddles} &\simeq 52\,YR_{Au+Au} + 4\,YR_{Beam\ Gas} + 2\,YR_{e+e-} && (45)\\
Y\#MIP_{paddles} &\simeq 4.2\times10^{14} && (46)\\
Y\#MIP_{rings} &\simeq 7\,YR_{Au+Au} + 4\,YR_{Beam\ Gas} + 1\,YR_{e+e-} && (47)\\
Y\#MIP_{rings} &\simeq 2.0\times10^{14} && (48)\\
Y\#MIP_{cement\ joints} &\simeq 2.0\times10^{14} && (49)
\end{aligned}
$$

assuming from the simulations that there are 52 particles hiting the paddles in average for each $Au+Au$ interaction, 4 hits from the beam gas and 2 particles fron the e+e- interactions.

The same for the ring conters and cement joins, 7 particles from $Au+Au$, 4 from beam gas and 1 from the e+e-.
The energy deposited per MIP in the paddles (ΔE) is $\simeq$ 1.7 MeV, in the rings $\simeq$ 7.5 MeV, and in the cement joints $\simeq$ 0.05 MeV. The mass of the paddles is $\simeq$ 136, of the rings $\simeq$ 20.0 g, and of the cement joints $\simeq$ 0.5 g. 1 rad $= 6.24\times10^7$ MeV/g, the dose rate will be:

$$
\begin{aligned}
YD &\simeq 1.60\times10^{-8}\,Y\#MIP\ \Delta E\ mass && (50)\\
YD_{paddles} &\simeq 8.4\times10^{4}\,\frac{rad}{year} && (51)\\
YD_{rings} &\simeq 1.2\times10^{6}\,\frac{rad}{year} && (52)\\
YD_{cement\ joints} &\simeq 3.2\times10^{5}\,\frac{rad}{year} && (53)
\end{aligned}
$$

These materials (BC-800 UVT rings, BC-600 optical cement, and BC-404 plastic scintillators) are slightly damaged (10 % loss of transparency) when exposed to about 1 Mrad [8]. It is expected that RHIC will be performing at about 1/6, 1/2 and 1/2 of full luminosity per year the first three years, so that the effects of radiation will be noticeable only after 3 years.

References

[1] B. Wyslouch *Nuclear Physics* **A566** (1994) 305c.

[2] T. Ludlam *et. al.*, *Proceedings of RHIC Workshop I*, Brookhaven National Laboratory, Ed. P. Haustein and C. Woody, **BNL-51921**, 1985.

[3] *Proceedings of the Second Workshop on Machine Backgrounds at RHIC*, Brookhaven National Laboratory. Ed. S. White, 1986.

[4] *RHIC Design Manual* Brookhaven National Laboratory, Upton NY, 1996.

[5] J. S. Wu *et. al., Nucl. Inst. and Meth.* **A311** (1992) 249.

[6] M. J. Rhoades-Brown and J. Weneser., *Phys. Rev.* **A** 44 (1991) 130.

[7] C. F. Maguire et. al. *A Primer for the PHENIX Simulation Codes PISA and PISORP, With an Introduction to PAUDA Version 3.1*, Internal **PHENIX** Document, February 1997.

[8] *Radiation Effects at the SSC*, SSC Central Design Group, **SSC-SR-1053**. M.G.D. Gilchriese Editor, Berkeley CA. 1988.